Supporting Information

Controlled charge injection into nitrogen for efficient electrochemical nitrogen reduction based on metal-on-boron compound catalysts

Yunji Han,[†a,b] Mihyeon Jo,[†a,b] Hyung-Kyu Lim*[c] and Sangheon Lee*[a,b]

[a.] Department of Chemical Engineering and Materials Science, Ewha Womans University, 52, Ewhayeodae-gil, Seodaemun-gu, Seoul 03760, Republic of Korea

[b.] Graduate Program in System Health Science and Engineering, Ewha Womans University, 52, Ewhayeodae-gil, Seodaemun-gu, Seoul 03760, Republic of Korea

[c.] Division of Chemical Engineering and Bioengineering, Kangwon National University, Chuncheon, Gangwon-do 24341, Republic of Korea

* Corresponding authors: hklim@kangwon.ac.kr (H.-K.L.), sang@ewha.ac.kr (S.L.)

† The two authors are equally contributed.

Table S1. The vibrational and solvation energy quantities for dual Ru doped models.

Model	α-sheets			β₁₂-sheets		
	ΔE_{vib} (kcal/mol)	ΔS_{vib} (cal/mol·K)	ΔG_{solv} (kcal/mol)	ΔE_{vib} (eV)	ΔS_{vib}	ΔG_{solv}
*	-	-	−4.93	-	-	−4.99
*N$_2$	6.02	7.21	−2.77	5.55	11.13	−3.30
*N$_2$H	12.78	7.30	−5.54	12.63	9.87	−6.05
*N$_2$H$_2$	20.35	8.32	−6.16	19.94	11.21	−6.75
*N$_2$H$_3$	27.28	8.69	−7.45	27.33	10.73	−9.70
*N$_2$H$_4$	33.50	16.66	−7.44	32.76	15.46	−7.34
*NH$_2$	16.64	10.49	−6.13	16.69	9.78	−6.25

Table S2. Structural information of catalyst models for DACs. The formation energy of DACs (ΔE_f) is calculated using $\Delta E_f = E_{TMs/Boron} - E_{TMs} - E_{Boron}$, where, $E_{TMs/Boron}$, E_{TMs}, and E_{Boron} represent the energy of the metal-embedded boron sheet, the bulk metal, and the boron sheet, respectively. Distances between the active site and the boron sheet, as well as between two TMs, are listed as d_{M-B} and d_{M-M}, respectively. Cd and Zn adsorbed on α-sheets do not exhibit stable binding states.

TMs	α-sheets			β_{12}-sheets		
	ΔE_f (eV)	d_{M-B} (Å)	d_{M-M} (Å)	ΔE_f (eV)	d_{M-B} (Å)	d_{M-M} (Å)
Ag	1.138	2.452	5.132	0.558	2.548	2.913
Cd	-	-	-	0.149	2.751	2.840
Co	0.504	1.845	5.132	0.031	1.907	2.948
Cr	1.721	2.246	5.131	0.845	2.287	2.883
Cu	0.917	2.088	5.132	0.368	2.182	2.676
Fe	0.945	1.988	5.133	0.470	2.046	2.834
Mn	0.954	2.044	5.132	0.037	2.160	2.917
Mo	2.439	2.125	5.132	1.369	2.188	2.294
Nb	2.192	2.183	5.131	0.679	2.168	2.878
Ni	0.399	1.922	5.132	0.382	2.099	2.525
Pd	0.598	2.287	5.132	0.179	2.335	2.800
Rh	0.979	2.198	5.131	0.693	2.198	2.749
Ru	1.837	2.148	5.139	1.402	2.165	2.526
Tc	2.164	2.118	5.132	1.368	2.144	2.527
Ti	1.510	2.138	5.131	-0.301	2.141	2.918
V	1.734	2.083	5.133	0.146	2.043	2.923
Zn	-	-	-	0.241	2.338	2.670
Zr	1.790	2.284	5.128	-0.163	2.273	3.056

Table S3. The formation energy of SACs on CeO_2 (111), α-sheet, $β_{12}$-sheet. The formation energy of SACs (ΔE_f) is calculated using $\Delta E_f = E_{TM/Substrate} - E_{TM} - E_{Substrate}$, where, $E_{TM/Substrate}$, E_{TM}, and $E_{Subsrate}$ represent the energy of the metal-embedded substrate, the bulk metal, and the substrate, respectively. (unit: eV)

ΔE_f	CeO_2	α-sheets	$β_{12}$-sheets
Pd	1.523	0.530	0.255
Pt	1.158	0.388	0.018
Ru	4.340	1.769	1.498

Table S4. Metal-metal distances (d_{M-M}) of side-on N_2 adsorption structures with negative binding free energy. (unit: Å)

TMs	α-sheets	β$_{12}$-sheets
Cr	4.557	2.640
Mn	4.570	2.725
Mo	4.542	2.697
Nb	4.660	2.875
Ni	4.468	-
Rh	4.527	2.841
Ru	4.452	-
Tc	4.406	2.641
Ti	4.629	2.822
V	4.543	2.700
Zr	4.752	3.009

Table S5. Average partial charge values at each TMs of bare catalyst based on the Bader charge analysis. (unit: $|e|$)

TMs	α-sheets	β_{12}-sheets
Ag	0.228	0.261
Cd	-	0.345
Co	−0.098	0.129
Cr	0.700	0.692
Cu	0.285	0.294
Fe	0.387	0.511
Mn	0.561	0.692
Mo	0.568	0.510
Nb	0.944	0.985
Ni	0.224	0.219
Pd	−0.046	−0.042
Rh	−0.084	−0.030
Ru	0.198	0.231
Tc	0.254	0.284
Ti	1.096	0.945
V	0.898	0.805
Zn	-	0.444
Zr	1.194	1.039

Table S6. Average partial charge values at each TMs and average partial charge values of N for N$_2$ adsorbed catalyst based on the Bader analysis method. (unit: $|e|$)

TMs	α-sheets		β$_{12}$-sheets	
	@TMs	@N	@TMs	@N
Ag	0.365	-0.134	0.333	-0.042
Cd	-	-	0.595	-0.128
Co	0.377	-0.170	0.349	-0.111
Cr	0.949	-0.378	1.000	-0.386
Cu	0.387	-0.074	0.370	-0.049
Fe	0.445	-0.144	0.411	-0.096
Mn	0.776	-0.285	0.908	-0.334
Mo	0.856	-0.389	0.962	-0.428
Nb	1.305	-0.458	1.585	-0.516
Ni	0.189	-0.107	0.336	-0.133
Pd	0.156	-0.155	0.122	-0.076
Rh	0.137	-0.217	0.239	-0.224
Ru	0.313	-0.304	0.319	-0.235
Tc	0.545	-0.386	0.648	-0.399
Ti	1.314	-0.470	1.353	-0.411
V	1.126	-0.393	1.207	-0.416
Zn	-	-	0.684	-0.171
Zr	1.615	-0.637	1.672	-0.500

Table S7. Average partial charge values of N_2 molecule adsorbed on DACs , corresponding N_2 adsorption free energies, and COHP-calculated metal-N_2 binding strength (denoted as ICOHP@E_F).

TMs	Partial charge @ N (|e|)		ΔG_{N2} (eV)		ICOHP@E_F (eV)	
	α	β_{12}	α	β_{12}	α	β_{12}
Ag	-0.134	-0.042	0.54	0.47	-2.00	-1.61
Cd		-0.128		0.79		-1.08
Co	-0.170	-0.111	0.28	0.99	-3.18	-2.83
Cr	-0.378	-0.386	-0.55	-0.73	-2.82	-2.43
Cu	-0.074	-0.049	0.26	0.14	-2.23	-2.16
Fe	-0.144	-0.096	0.07	-0.44	-2.65	-2.61
Mn	-0.285	-0.334	-0.24	-0.08	-2.27	-1.83
Mo	-0.389	-0.428	-1.05	-0.91	-3.22	-2.77
Nb	-0.458	-0.516	-1.12	-1.30	-3.83	-2.79
Ni	-0.107	-0.133	-0.10	-0.16	-2.55	-2.56
Pd	-0.155	-0.076	0.13	0.22	-1.94	-2.19
Rh	-0.217	-0.224	-0.28	-0.13	-2.36	-2.34
Ru	-0.304	-0.235	-0.28	-0.36	-2.89	-2.05
Tc	-0.386	-0.399	-1.23	-0.81	-3.43	-3.24
Ti	-0.470	-0.411	-1.41	-1.49	-3.02	-2.02
V	-0.393	-0.416	-1.00	-0.77	-2.86	-2.26
Zn		-0.171		0.44		-1.63
Zr	-0.637	-0.500	-1.74	-1.56	-4.12	-2.60

Table S8. Differences (denoted as Δq @ TM) in the average partial charge value at each TM after and before the N_2 adsorption. Average partial charge values (denoted as q @ N) of N for N_2 adsorbed catalyst. Calculations are based on the Bader analysis method. (unit: $|e|$)

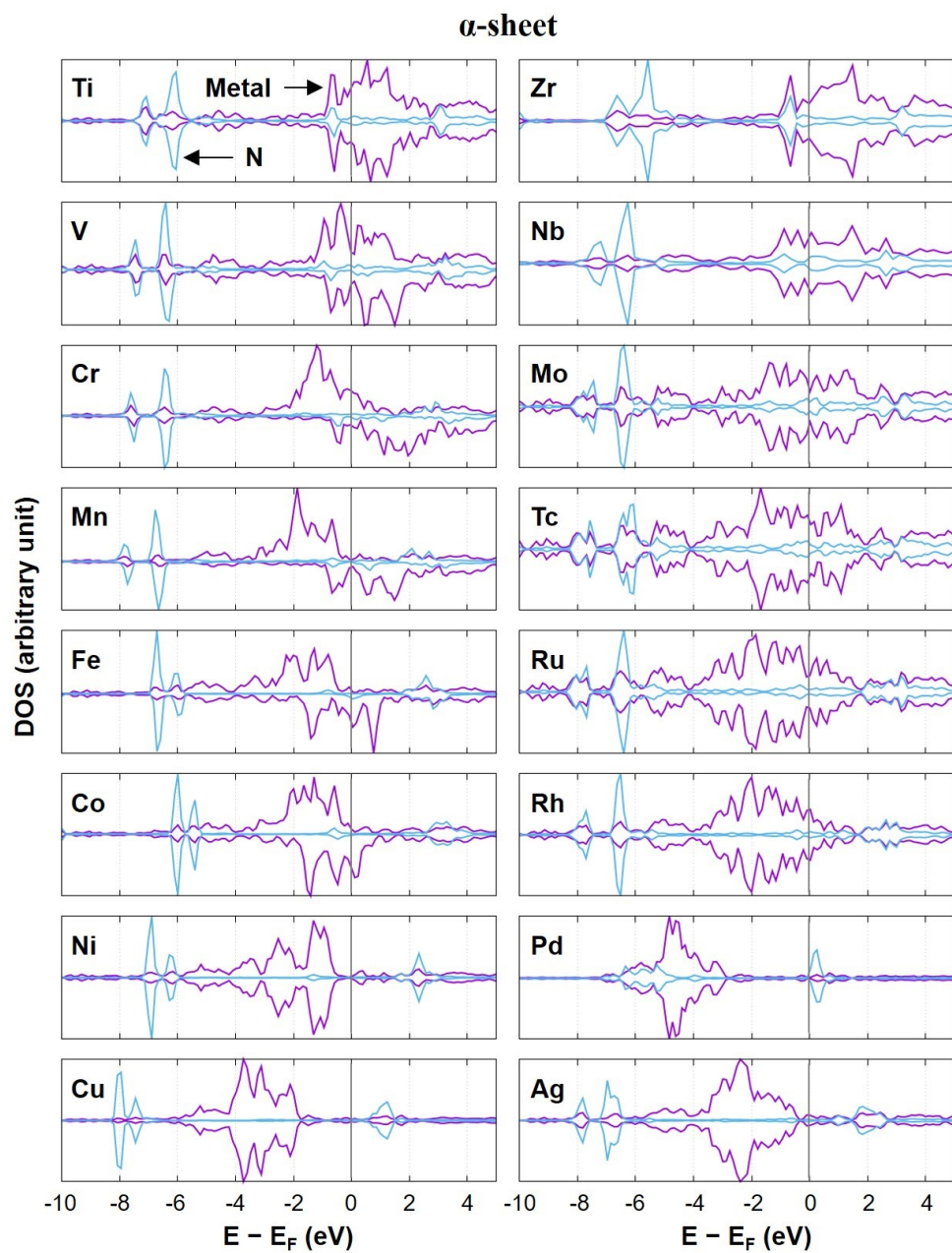|	Δq @ TM		q @ N	
	α	β_{12}	α	β_{12}
Ag	0.137	0.072	-0.134	-0.042
		0.250		-0.128
Co	0.475	0.220	-0.170	-0.111
Cr	0.249	0.308	-0.378	-0.386
Cu	0.102	0.076	-0.074	-0.049
Fe	0.058	-0.100	-0.144	-0.096
Mn	0.215	0.216	-0.285	-0.334
Mo	0.288	0.452	-0.389	-0.428
Nb	0.361	0.600	-0.458	-0.516
Ni	-0.035	0.117	-0.107	-0.133
Pd	0.202	0.164	-0.155	-0.076
Rh	0.221	0.269	-0.217	-0.224
Ru	0.115	0.088	-0.304	-0.235
Tc	0.291	0.364	-0.386	-0.399
Ti	0.218	0.408	-0.470	-0.411
V	0.228	0.402	-0.393	-0.416
		0.240		-0.171
Zr	0.421	0.633	-0.637	-0.500

Table S9. Average partial charge value (unit: $|e|$) at each TM (denoted as q @ TM) on bare α- and β$_{12}$-sheets and calculated H$_2$O adsorption free energies (denoted as ΔG_{H2O}) (unit: eV).

	q @ TM		ΔG_{H2O}	
	α	β$_{12}$	α	β$_{12}$
Ag	0.228	0.261	0.294	0.681
Cd		0.345		0.293
Co	-0.098	0.129	0.154	0.005
Cr	0.700	0.692	0.044	-0.054
Cu	0.285	0.294	0.224	-0.002
Fe	0.387	0.511	0.147	-0.160
Mn	0.561	0.692	0.009	-0.097
Mo	0.568	0.51	0.046	0.280
Nb	0.944	0.985	-0.621	-0.161
Ni	0.224	0.219	0.178	0.050
Pd	-0.046	-0.042	0.402	0.055
Rh	-0.084	-0.03	0.320	0.121
Ru	0.198	0.231	0.242	0.146
Tc	0.254	0.284	0.260	0.137
Ti	1.096	0.945	-0.782	-0.417
V	0.898	0.805	-0.364	-0.021
Zn		0.444		0.048
Zr	1.194	1.039	-1.252	-0.261

Bare TMs@α-sheet

*N$_2$ TMs@α-sheet

Contraction of
TMs distance

Boron sheet corrogation
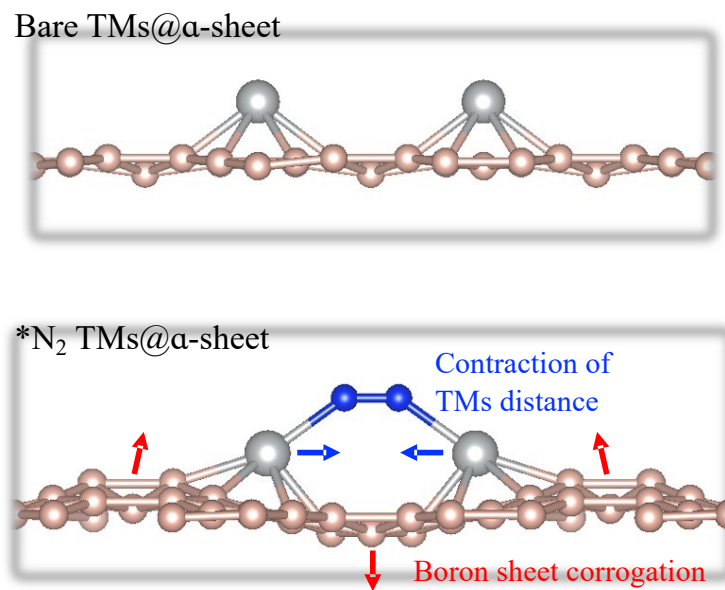
Figures S1. Structural changes of TMs on α-sheet after side-on N$_2$ adsorption.

α-sheet

Figures S2. Partial density of states (pDOS) analysis of N_2 and TMs on α-sheets for the most stable N_2 adsorption structures (see **Figure 1**).
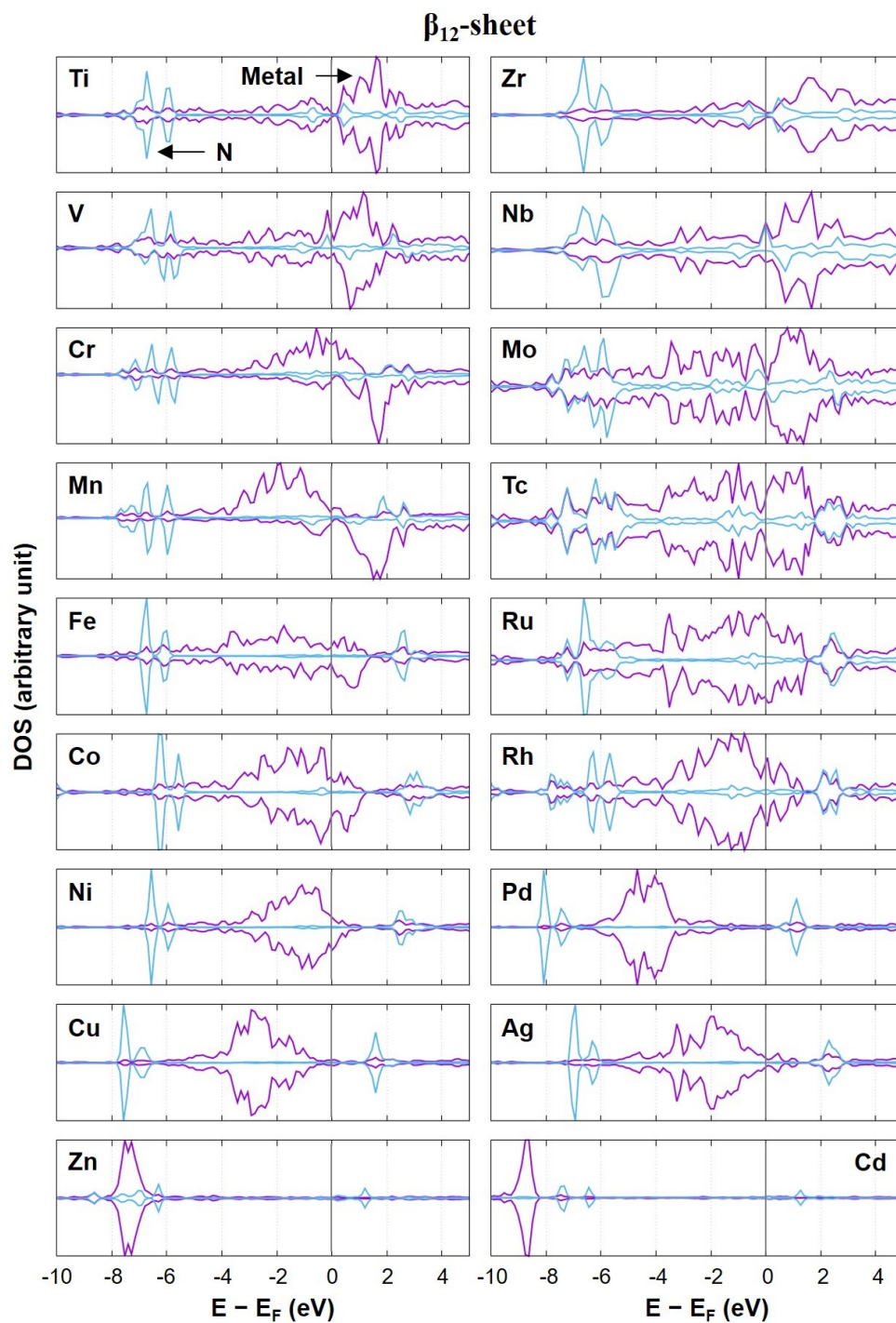
β₁₂-sheet

Figures S3. Partial density of states (pDOS) analysis of N_2 and TMs on β₁₂-sheets for the most stable N_2 adsorption structures (see **Figure 1**).
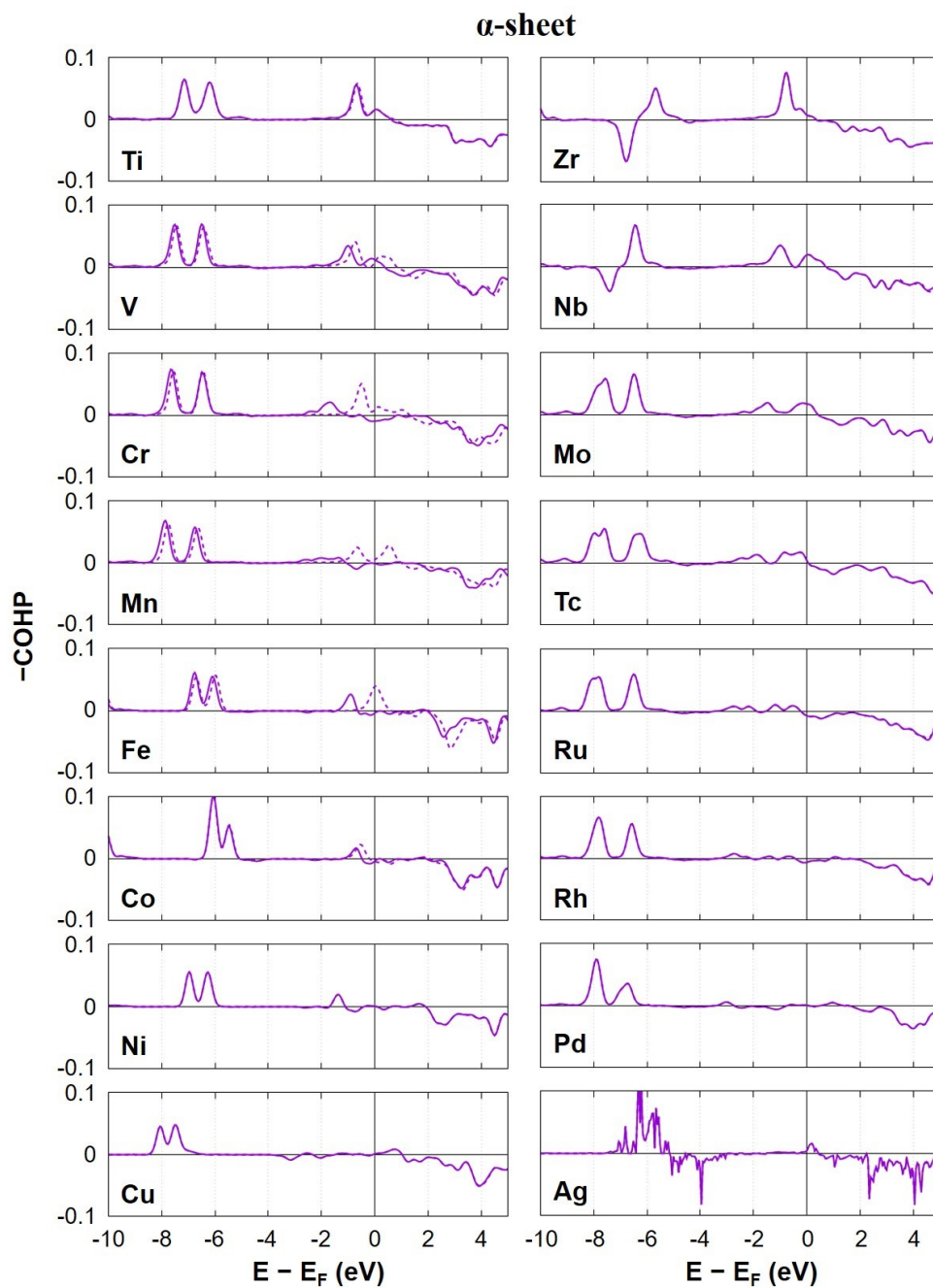
α-sheet

Figures S4. Crystal orbital Hamiltonian projection (COHP) analysis of TM-N_2 bonding on α-sheets for the most stable N_2 adsorption structures (see **Figure 1**). Solid and dot lines denote spin-up and spin-down states, respectively.
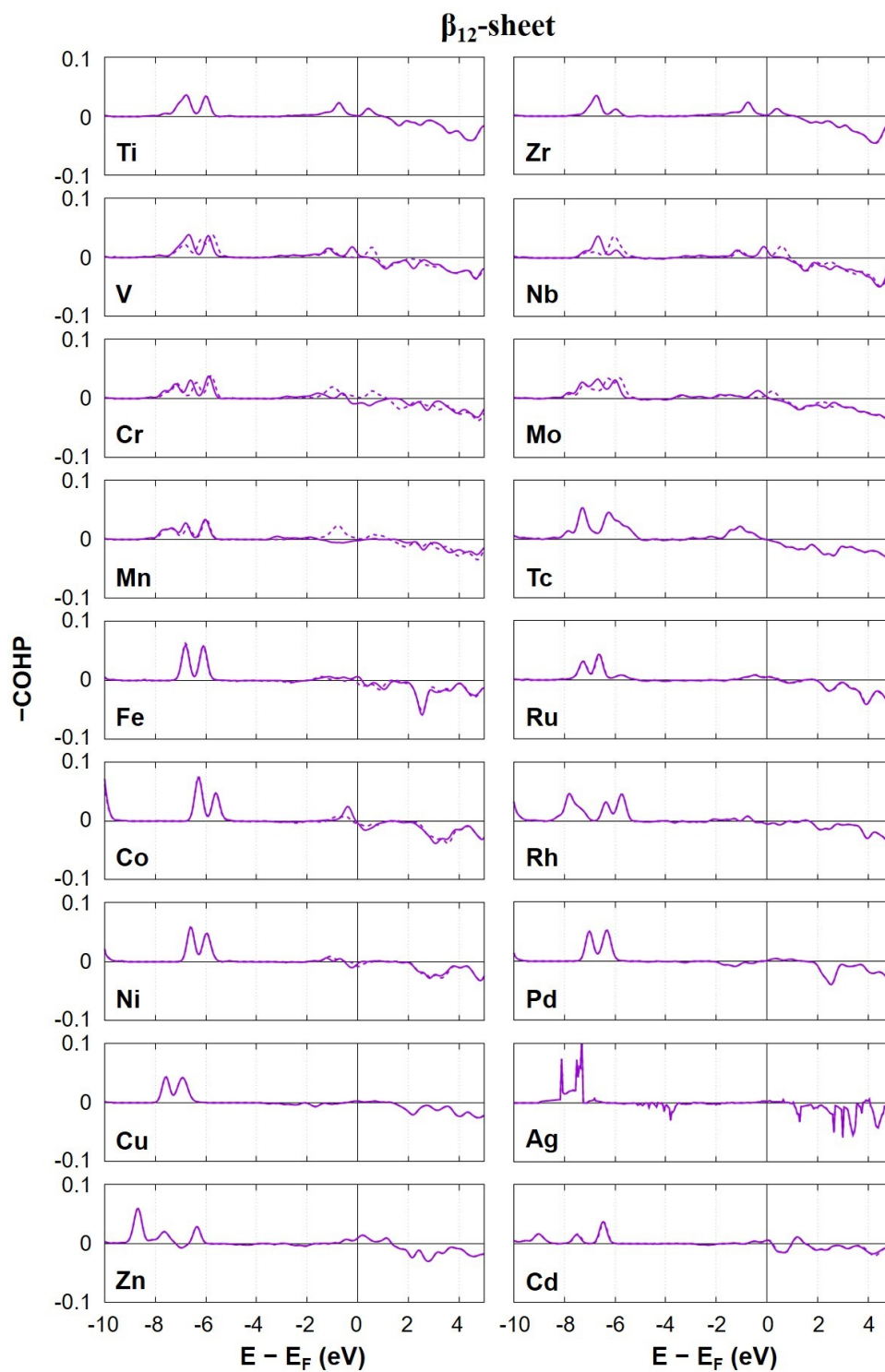
Figures S5. Crystal orbital Hamiltonian projection (COHP) analysis of TM-N_2 bonding on β_{12}-sheets for the most stable N_2 adsorption structures (see **Figure 1**). Solid and dot lines denote spin-up and spin-down states, respectively.
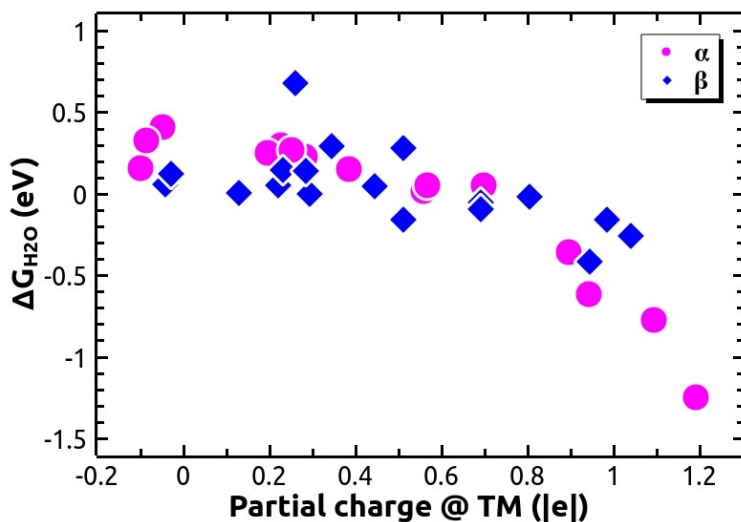
Figures S6. Calculated H_2O adsorption free energies as a function of the partial charge at TM on α-sheets (denoted as α) and $β_{12}$-sheets (denoted as β). Calculations of the partial charge are based on the Bader analysis method. Refer to raw data in **Table S9**.
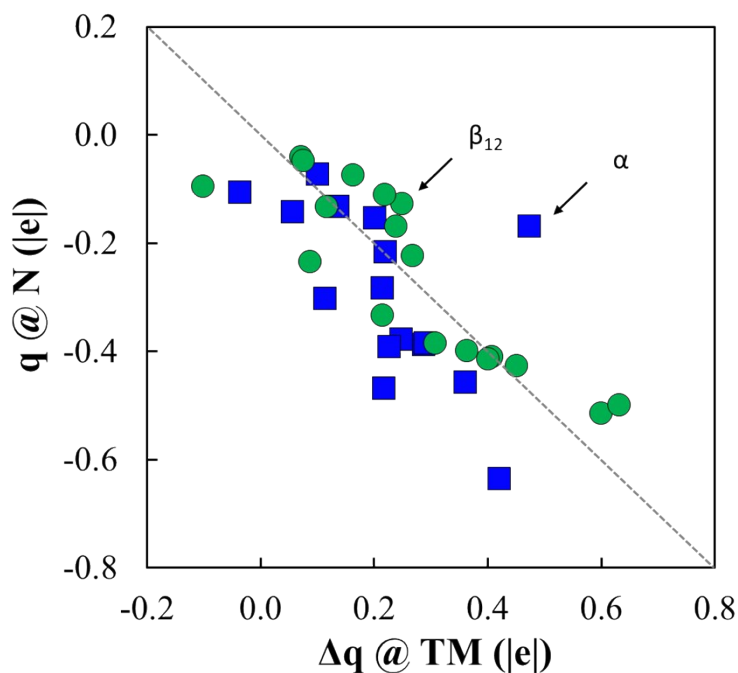
Figures S7. Correlation between differences (denoted as $Δq$ @ TM) in the average partial charge value at each TM after and before the N_2 adsorption and average partial charge values (denoted as q @ N) of N for N_2 adsorbed catalyst. Calculations are based on the Bader analysis method. Refer to raw data in **Table S8**. (unit: $|e|$)
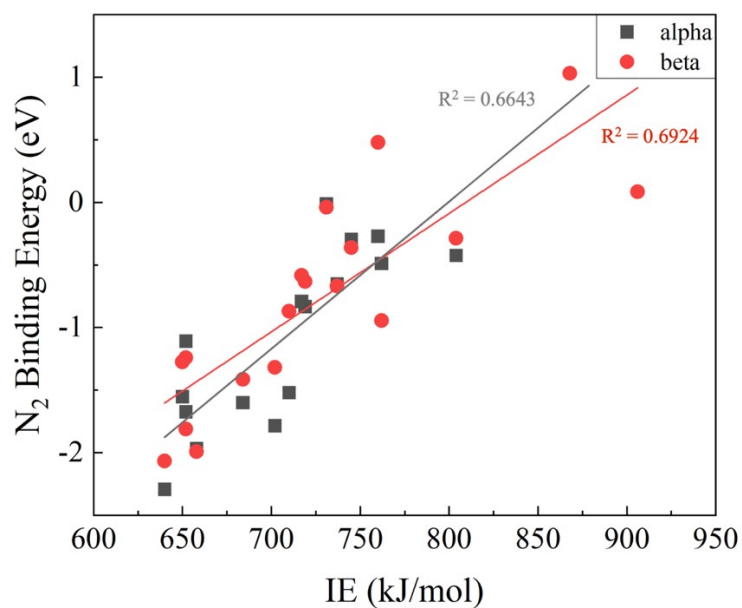
Figure S8. Correlation between TMs 1st electron ionization energy (source: https://ptable.com) and N_2 binding energy.
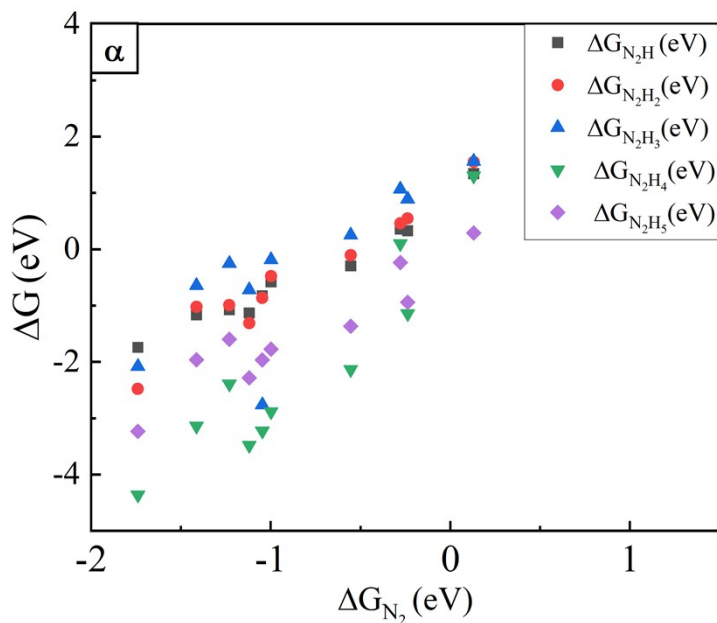
Figure S9. Linear correlations between binding free energies of N_2 and N_2H, N_2H_2, N_2H_3, N_2H_4, N_2H_5 for TMs on α-sheet.
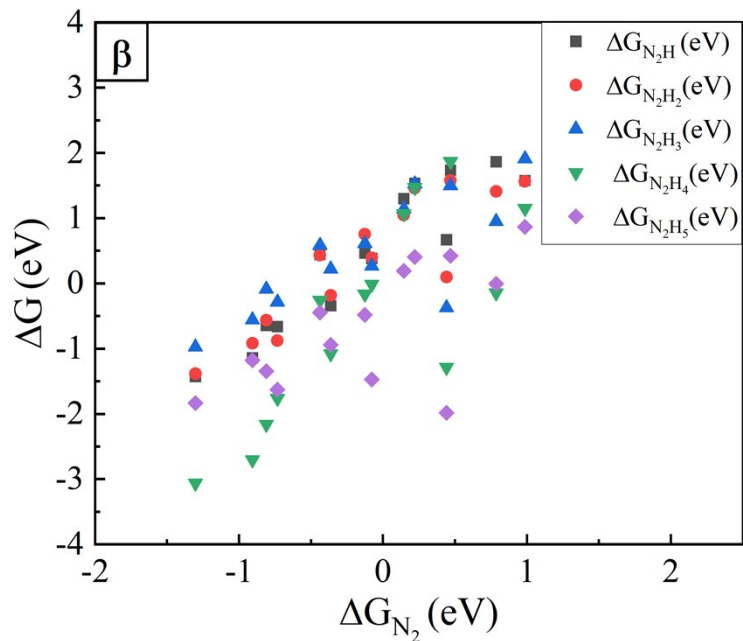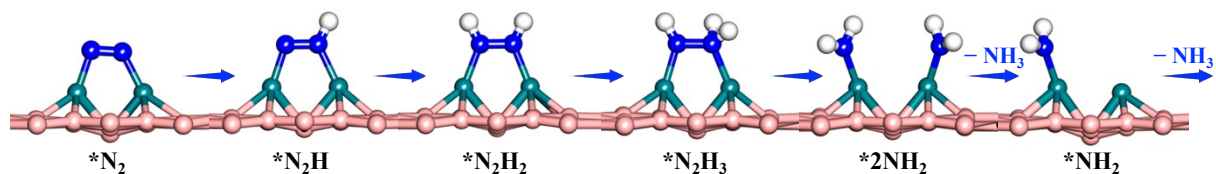
Figure S10. Linear correlations between binding free energies of N_2 and N_2H, N_2H_2, N_2H_3, N_2H_4, N_2H_5 for TMs on β_{12}-sheet.
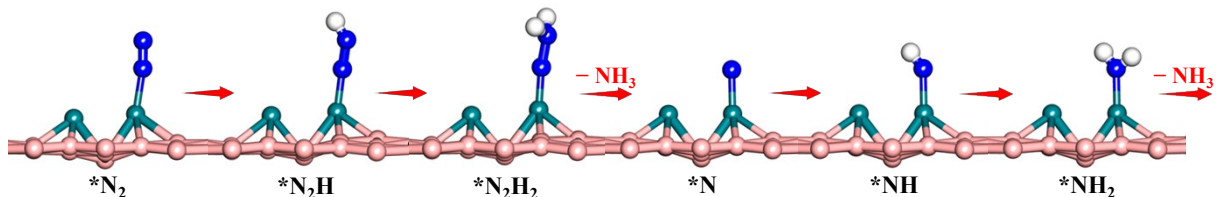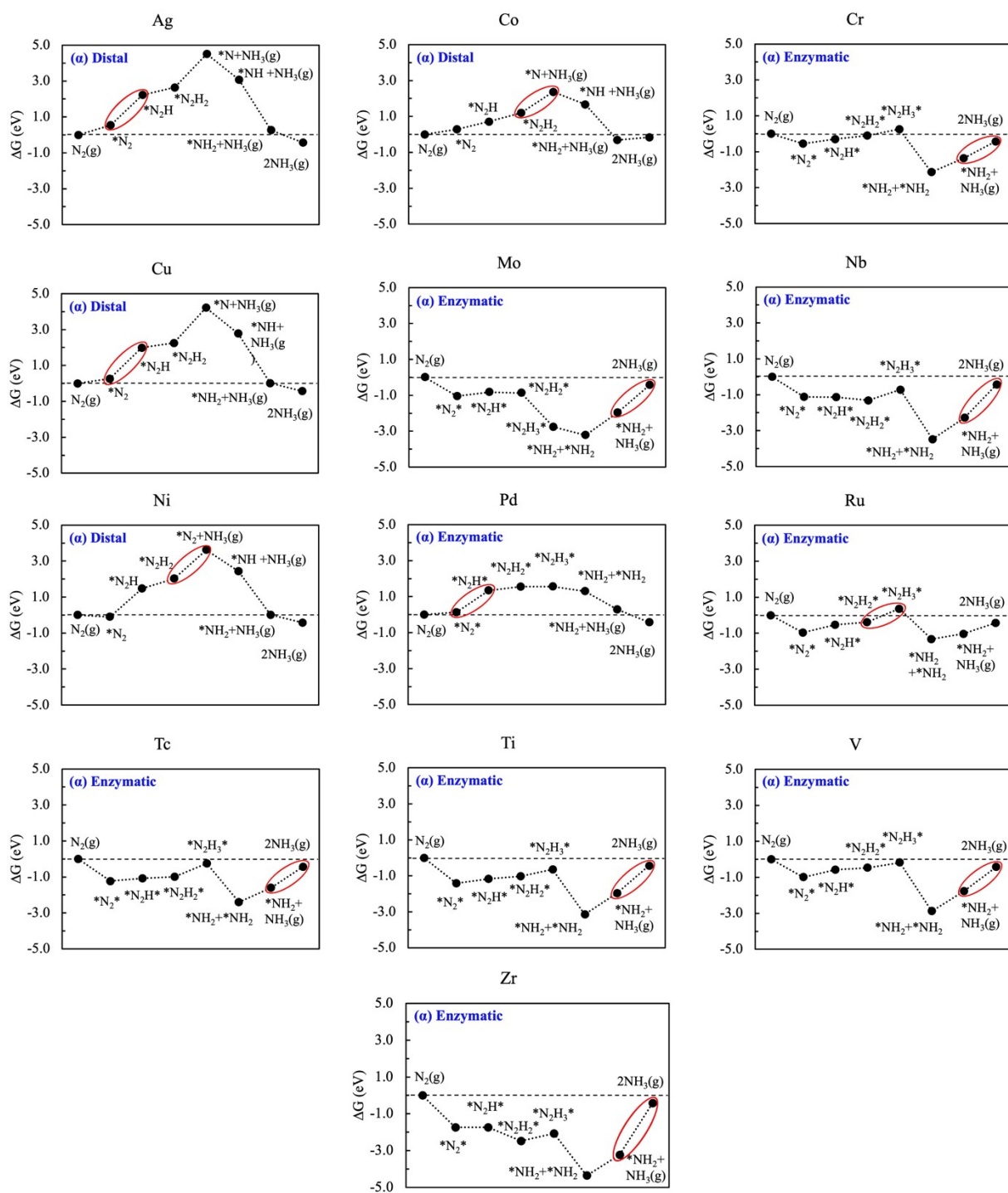

Figure S11. Conventional reaction pathways for eNRR.

Figure S12. Gibbs free energy profiles for overall eNRR pathway on TMs@α-sheet.
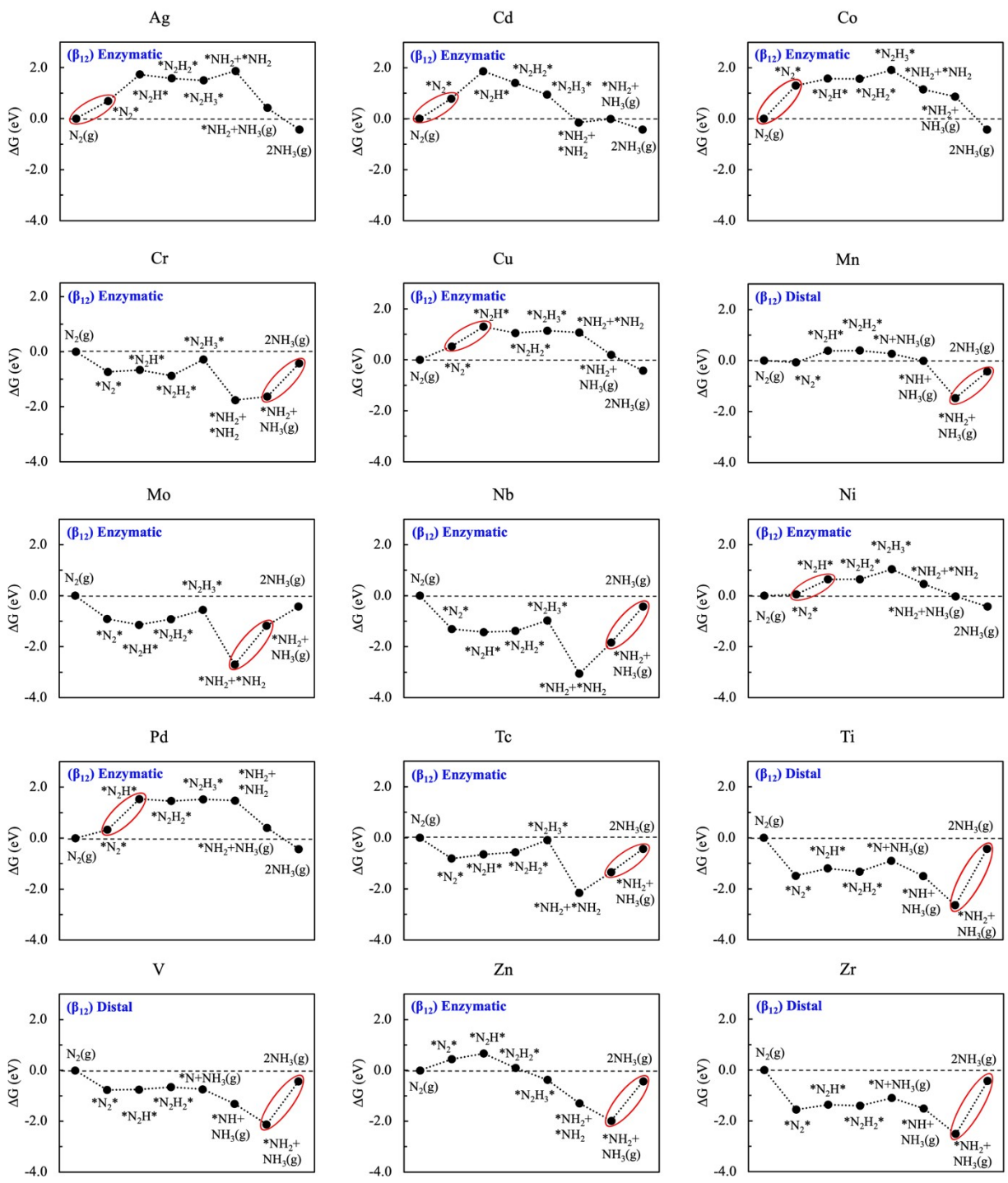
Figure S13. Gibbs free energy profiles for overall eNRR pathway on TMs@β_{12}-sheet.